Eur. Phys. J. C 49, 375–378 (2007)
DOI 10.1140/epjc/s10052-006-0085-6

THE EUROPEAN PHYSICAL JOURNAL C

Regular Article – Experimental Physics

Suppression of high-p_{T} non-photonic electrons in $\mathrm{Au}+\mathrm{Au}$ collisions at $\sqrt{s_{NN}} = 200\,\mathrm{GeV}$

J. Bielcik[a] for the STAR Collaboration

Yale University, New Haven, CT 06520, USA

Received: 11 August 2006 /
Published online: 27 October 2006 –

Abstract. The strong suppression of high p_{T} hadrons observed at RHIC has led to the interpretation that energetic partons lose their energy via induced gluon radiation in the hot and dense matter before fragmenting into hadrons. The study of heavy quark production can extend our understanding of this scenario. Due to the dead cone effect, the suppression of heavy quark mesons at high p_{T} is expected to be smaller than that observed for charged hadrons at the same energy. The measurement of non-photonic single electrons up to high p_{T} provides information on charm and beauty production. The semi-leptonic decays of D and B mesons are the dominant contribution to the non-photonic electron spectra. The preliminary spectra from $p+p$, $d+\mathrm{Au}$ and $\mathrm{Au}+\mathrm{Au}$ collisions at $\sqrt{s_{NN}} = 200$ GeV have been extracted for mid-rapidity non-photonic electrons in the range $1.5 < p_{\mathrm{T}}\,(\mathrm{GeV}/c) < 10$. The corresponding nuclear modification factors (R_{AA}) are presented and show a large suppression in central $\mathrm{Au}+\mathrm{Au}$ collisions, indicating an unexpectedly large energy loss for heavy quarks in the hot and dense matter created at RHIC. This observed suppression is compared to recent theoretical models.

PACS. 13.85.Qk; 13.20.Fc; 13.20.He; 25.75.Dw

1 Introduction

The observation of the suppression of inclusive high-p_{T} hadron yields in central $\mathrm{Au}+\mathrm{Au}$ collisions at the Relativistic Heavy-Ion Collider (RHIC) [1–4] is one of the signatures of quark–gluon plasma production. The suppression is a consequence of medium induced radiative energy loss of energetic light partons, mainly gluons in the created nuclear matter. The amount of parton energy loss depends on the properties of the medium, such as gluon density, or the length that the parton travels in the medium. It also depends on the properties of the parton, such as color charge or mass. Therefore, it is possible to independently explore the properties of nuclear matter by measuring the energy loss of different types of partons. The heavy quarks (charm and beauty) are mostly produced in initial hard parton scattering through gluon fusion [5,6]. The suppression of high-p_{T} heavy quarks is also expected though smaller than for light quarks, due to reduction of small angle gluon radiation [7–9]. Because of the large quark masses, charm and beauty production can be calculated by perturbative QCD (pQCD) [10]. The cross-sections and p_{T} spectra were calculated in next-to-leading order (NLO) for both $p+p$ and $\mathrm{Au}+\mathrm{Au}$ collisions [11–13]. Although the calculations are in agreement with the data at the Tevatron at $\sqrt{s_{NN}} = 1.8$ TeV [14], they underestimate the production at RHIC [15,16].

The heavy quark meson production was studied directly by D^0 meson reconstruction via the hadronic decay: $D^0 \to K^-\pi^+$, in both $d+\mathrm{Au}$ [17] and $\mathrm{Au}+\mathrm{Au}$ [18] collisions. Due the statistical reconstruction of D^0, the measured spectra were limited to $p_{\mathrm{T}} < 3\,\mathrm{GeV}/c$. The reconstruction of non-photonic electrons is an alternative method to infer information about the heavy quark production and their interactions with the medium. The non-photonic electron spectra are dominated by semileptonic decays of D and B mesons. This method is presented here. There are several sources of measured electrons. We divide them into non-photonic electrons (signal) and photonic electrons (background). The background photonic electrons are from γ conversions, and π^0, η Dalitz and light vector meson decays.

2 Data analysis

The results presented in this paper were obtained from an analysis of data recorded with the STAR detector [19] in years 2003 ($p+p$, $d+\mathrm{Au}$) and 2004 ($\mathrm{Au}+\mathrm{Au}$). The two main detector systems used in the analysis were the Time Projection Chamber (TPC) and the Barrel Electromagnetic Calorimeter (BEMC), that also contains the

[a] e-mail: jaroslav.bielcik@yale.edu

Shower Maximum Detector (SMD). Part of the data were taken with a trigger based on energy deposited in a single tower of the BEMC. This enriched the high-p_T part of electron spectra. The integrated luminosity sampled by the EMC trigger is 100 nb^{-1} for $p+p$, 370 μb^{-1} for $d+$Au and 26 μb^{-1} for the most central Au + Au events.

The electron identification was based on a combination of energy loss ($\mathrm{d}E/\mathrm{d}x$) in the TPC, energy deposition E in the BEMC, and the shower profile in the SMD. For the details of the analysis see elsewhere [20, 21]. Reconstructed tracks that point to the primary vertex are selected in order to suppress conversion electrons. Tracks are projected to the BEMC and those with $p/E < 2$, where p is the reconstructed momentum, are chosen. Further selection is based on the shower size in the SMD. The tracks with a large shower size correspond to electrons. The final electron identification criterium is $\mathrm{d}E/\mathrm{d}x$. Electrons with momentum $1.5 < p < 10$ GeV/c lose average more energy in the TPC than other charged particles. Electrons are selected with $\mathrm{d}E/\mathrm{d}x_{\min} < \mathrm{d}E/\mathrm{d}x < 5.1$ keV/cm. $\mathrm{d}E/\mathrm{d}x_{\min}$ is around 3.5 keV/cm, with the specific value depending on the event multiplicity and increases slowly with track momentum to optimize electron efficiency and hadron rejection. The resulting hadron contamination in the electron sample is $3 \pm 3\%$ at 2 GeV/c and $22 \pm 5\%$ at 8 GeV/c.

The data sample for the Au + Au dataset was divided into 3 centrality bins (0–5%, 10–40%, and 40–80% of the total geometrical cross section). The electron reconstruction efficiency and acceptance were determined by embedding simulated electrons into real events and calculated for each centrality separately. For the most central events, the electron reconstruction efficiency increases with p_T up to 5 GeV/c and then remains constant at 40%.

The dominant sources of photonic electrons are γ conversions in the detector material, π^0 and η Dalitz decays. The contribution from other sources is negligible when compared to the systematic uncertainties. The photonic background was evaluated by identifying both the electron and positron from a conversion or a Dalitz pair. The invariant mass of these pairs is always smaller than the π^0 mass. The background was statistically subtracted. The efficiency of the photonic background rejection was determined by embedding π^0 into real events and is $56 \pm 6\%$ for the most central Au + Au events.

2.1 Non-photonic electron spectra

Figure 1 (taken from [20]) shows the background subtracted non-photonic electron spectra for $p+p$, $d+$Au and Au + Au collisions together with FONLL pQCD predictions. The error bars are statistical and the boxes show the systematic uncertainties. The measured non-photonic electron spectra cover the p_T range where the contribution from both charm and beauty is predicted to be important. The FONLL pQCD prediction is scaled by a factor of 5.5, corresponding to the ratio between the charm cross section measured by STAR [18] and the one calculated within FONLL pQCD [13, 14].

Figure 2 (taken from [20]), upper part, shows the ratio of the measured non-photonic electron yield for $p+p$ collisions to that calculated by FONLL pQCD. Since the ratio is almost p_T independent, the calculated spectrum describes the shape of the measured spectrum well, however the total yield is strongly underestimated. We would like to note that the contributions from both charm and beauty decays are necessary to describe the shape of the $p+p$ spectra, see also Fig. 1. The ratio is consistent with the ratio of the measured and calculated charm production cross section (dashed line at 5.5). The same ratio is

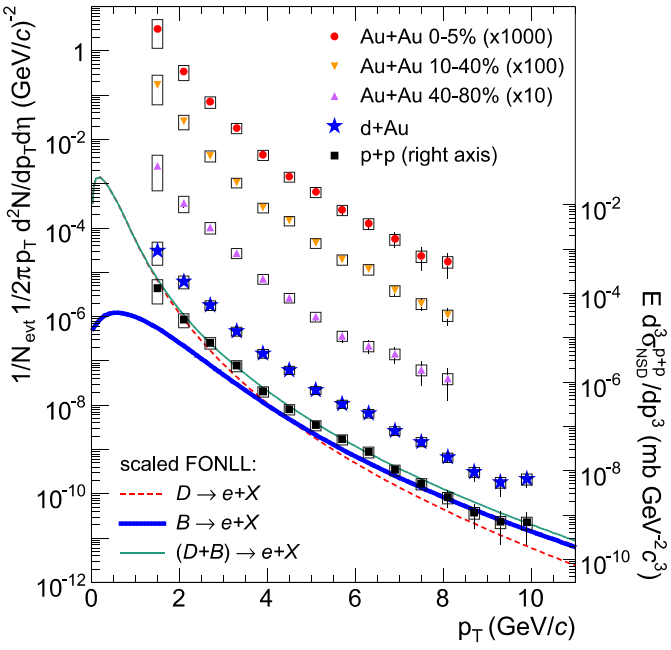

Fig. 1. Background subtracted non-photonic electron spectra for $p+p$, $d+$Au and Au + Au collisions for centralities 0–5%, 10–40% and 40–80%. The curves are scaled FONLL predictions for $p+p$ [13]. Cross section on the right axis applies to $p+p$ spectrum only

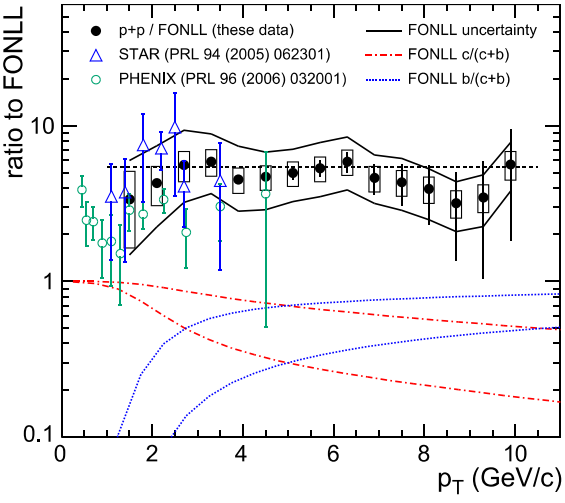

Fig. 2. *Upper*: ratio between measured non-photonic electron yield and FONLL pQCD calculations [13] for $p+p$ collisions; *lower*: relative contributions to FONLL distribution of c and b decays

also shown for previous STAR [17] and PHENIX [16] measurements. Within the experimental uncertainties, all the measurements are consistent.

Figure 2, lower part, shows the relative contribution of charm and beauty decays to the total spectrum of non-photonic electrons in the FONLL pQCD prediction with the variation due to uncertainties in the calculation. The calculation predicts that the amount of electrons from B meson decays becomes significant for $4 < p_{\mathrm{T}} < 6$ GeV/c. The crossing point where the beauty contribution start to dominate over charm is not well constrained due to uncertainties in the calculations. It can be as low as 3 GeV/c or as high as 10 GeV/c.

2.2 Nuclear modification factors, R_{AA}, for non-photonic electrons

Figure 3 (taken from [20]) shows the nuclear modification factors, R_{AA} and $R_{d\mathrm{Au}}$, for non-photonic electrons as a function of p_{T}. The error bars show the statistical uncertainties. The boxes show the uncorrelated systematic uncertainties, and the filled band is the overall normalization uncertainty, including the uncertainties in the number of binary collisions. R_{AA} ($R_{d\mathrm{Au}}$) is defined as the ratio of the spectra measured in Au + Au (d + Au) collisions to the spectrum measured in $p+p$ collisions scaled by the number of binary collisions in Au + Au (d + Au). In the absence of nuclear effects, $R_{AA} = 1$ ("binary scaling").

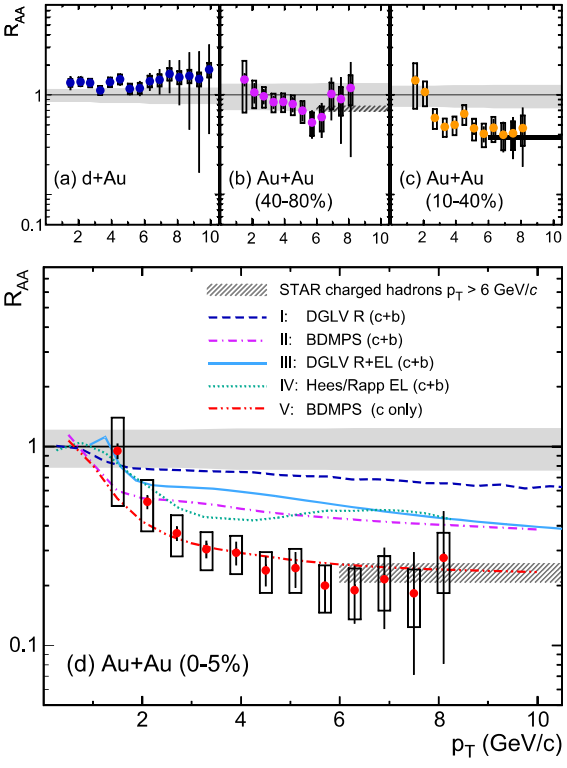

Fig. 3. The nuclear modification factor, R_{AA}, for d + Au and Au + Au collisions at $\sqrt{s_{NN}} = 200$ GeV. *Error bars* and uncertainties are described in text

The $R_{d\mathrm{Au}}$ ratio is consistent with a moderate Cronin enhancement, however a simple binary scaling with respect to $p+p$ collisions can not be ruled out. On the other hand, it is possible to observe an increased suppression from peripheral to central Au + Au events with respect to the binary scaling. The suppression reaches a factor of 5 for $p_{\mathrm{T}} > 4$ GeV/c. It is consistent with previous measurements at lower p_{T} [22, 23]. Assuming that a significant fraction of non-photonic electrons indeed comes from heavy quark meson decays, this suppression indicates a strong interaction and a large energy loss of heavy quarks in the medium created at RHIC. This suppression is as strong as the suppression observed for light hadrons for $p_{\mathrm{T}} > 6$ GeV/c [2].

2.3 Comparison of results with theoretical models

Figure 3 also shows calculations of the R_{AA} from three theoretical models. In all cases, the contribution from charm and bottom quarks were taken into account as it is calculated with FONLL pQCD [13] and final state energy loss was calculated.

In the first model (dashed curve)[8], the DGLV theory of radiative energy loss has been applied and the created nuclear matter is characterized by the initial gluon density of $\frac{\mathrm{d}N_{\mathrm{g}}}{\mathrm{d}y} = 1000$, the value derived from light quark hadron suppression. In addition, the contribution from elastic energy loss has been taken into account (solid line)[24]. Recently, the elastic energy loss has been reevaluated and for heavy quarks it is comparable to the radiative energy loss [8, 25].

In the second model (dash-dotted curve)[9], the medium is characterized by the time averaged BDMPS transport coefficient, $\hat{q} = 14\,\mathrm{GeV}^2/\mathrm{fm}$, for central Au + Au collisions. This value of $\hat{q}$ is consistent with the measurement of R_{AA} of the light hadrons, which restricts the value $\hat{q} = (4\text{–}14\,\mathrm{GeV}^2/\mathrm{fm})$ [27]. In this approach no contribution of elastic energy loss was taken into account. For the sake of comparison, a curve (dash-dot-dot) representing the contribution only from charm sources is shown.

In the third model (dotted curve)[28], the authors focus on elastic scattering of heavy quarks in the medium mediated by resonance excitations (D and B) off light quarks as well as by t-channel gluon exchange.

The measured data points of R_{AA} do not agree with the model calculations at high p_{T} if contributions from both beauty and charm sources is taken into account. The models predict a smaller suppression than that measured. However, if only the contribution from charm decays is considered then the models would agree well with the data. It is important to note that the model calculations also have large uncertainties, such as the amount of relative contribution from beauty/charm decays, that influence the final R_{AA}. Another issue is that the measured charm cross-section and also non-photonic electron spectra in $p+p$ collisions are about a factor of ≈ 5.5 higher than FONLL predictions. In addition, further understanding of $p+p$ collisions is necessary before we can make a final statement about heavy quark energy loss.

3 Summary

The non-photonic electron spectra for $p+p$, $d+$Au and Au + Au collisions at $\sqrt{s_{NN}} = 200$ GeV have been presented. The strong suppression of the spectra in central Au + Au collisions is observed, which suggests a strong energy loss of heavy quarks in nuclear matter. The theoretical models do not describe the data if both the charm and beauty contributions are accounted for. The FONLL pQCD calculations underestimate the measured spectra in $p+p$ by a factor of 5.5. The results raise the question about the predicted yields and the understanding of energy loss of heavy quarks, e.g. the contribution of beauty decays in the measured non-photonic electron spectra.

Acknowledgements. We thank the RHIC Operations Group and RCF at BNL, and the NERSC Center at LBNL for their support. This work was supported in part by the HENP Divisions of the Office of Science of the U.S. DOE; the U.S. NSF; the BMBF of Germany; IN2P3, RA, RPL, and EMN of France; EPSRC of the United Kingdom; FAPESP of Brazil; the Russian Ministry of Science and Technology; the Ministry of Education and the NNSFC of China; IRP and GA of the Czech Republic, FOM of the Netherlands, DAE, DST, and CSIR of the Government of India; Swiss NSF; the Polish State Committee for Scientific Research; STAA of Slovakia, and the Korea Sci. & Eng. Foundation.

References

1. STAR Collaboration, C. Adler et al., Phys. Rev. Lett. **89**, 202 301 (2002)
2. STAR Collaboration, J. Adams et al., Phys. Rev. Lett. **91**, 172 302 (2003)
3. PHENIX Collaboration, K. Adcox et al., Phys. Rev. Lett. **88**, 022 301 (2002) [nucl-ex/0109003]
4. PHENIX Collaboration, S.S. Adler et al., Phys. Rev. Lett. **91**, 072 301 (2003) [nucl-ex/0304022]
5. Z.W. Lin, M. Gyulassy, Phys. Rev. Lett. **77**, 1222 (1996)
6. Z.W. Lin, M. Gyulassy, Heavy Ion Phys. **4**, 123 (1996) [nucl-th/9510041]
7. Y.L. Dokshitzer, D.E. Kharzeev, Phys. Lett. B **519**, 199 (2001)
8. M. Djordjevic, M. Gyulassy, R. Vogt, S. Wicks, Phys. Lett. B **632**, 81 (2006) [nucl-th/0507019]
9. N. Armesto, M. Cacciari, A. Dainese, C.A. Salgado, U.A. Wiedemann, Phys. Lett. B **637**, 362 (2006) [hep-ph/0511257]
10. M.L. Mangano, P. Nason, G. Ridolfi, Nucl. Phys. B **405**, 507 (1993)
11. S. Frixione, M.L. Mangano, P. Nason, G. Ridolfi, Adv. Ser. Direct. High Energy Phys. **15**, 609 (1998) [hep-ph/9702287]
12. R. Vogt, Heavy Ion Phys. **18**, 11 (2003) [hep-ph/0205330]
13. M. Cacciari, P. Nason, R. Vogt, Phys. Rev. Lett. **95**, 122 001 (2005) [hep-ph/0502203]
14. S. Frixione, Eur. Phys. J. C **43**, 103 (2005)
15. J. Adams et al., Phys. Rev. Lett. **94**, 062 301 (2005)
16. S.S. Adler et al., Phys. Rev. Lett. **96**, 032 001 (2006)
17. STAR Collaboration, J. Adams et al., Phys. Rev. Lett. **94**, 062 301 (2005) [nucl-ex/0407006]
18. H. Zhang, nucl-ex/0510063
19. K.H. Ackermann et al., Nucl. Instrum. Methods A **499**, 624 (2003)
20. STAR Collaboration, B.I. Abelev, nucl-ex/0607012, submitted to Phys. Rev. Lett.
21. STAR Collaboration, J. Bielcik, nucl-ex/0511005
22. S.S. Adler et al., Phys. Rev. Lett. **96**, 032 301 (2006)
23. H. Zhang, nucl-ex/0607031
24. S. Wicks, W. Horowitz, M. Djordjevic, M. Gyulassy, nucl-th/0512076
25. M.G. Mustafa, Phys. Rev. C **72**, 014 905 (2005)
26. M. Djordjevic, nucl-th/0603066
27. A. Dainese, C. Loizides, G. Paic, Eur. Phys. J. C **38**, 461 (2005) [hep-ph/0406201]
28. H. van Hess, V. Greco, R. Rapp, Phys. Rev. C **73**, 034 913 (2006) and private comunication